Available online at www.sciencedirect.com
ScienceDirect
Developmental Biology 313 (2008) 196–209
DEVELOPMENTAL BIOLOGY
www.elsevier.com/developmentalbiology

Membrane-type MMPs enable extracellular matrix permissiveness and mesenchymal cell proliferation during embryogenesis

Joanne Shi, Mi-Young Son, Susan Yamada, Ludmila Szabova, Stacie Kahan [1], Kaliopi Chrysovergis [2], Lauren Wolf [3], Andrew Surmak, Kenn Holmbeck *

Matrix Metalloproteinase Unit, Craniofacial and Skeletal Diseases Branch, National Institute of Dental and Craniofacial Research, NIH, Bldg. 30, Room 125, 30 Convent Drive, MSC 4380, Bethesda, MD 20892-4380, USA

Received for publication 27 April 2007; revised 6 October 2007; accepted 16 October 2007
Available online 23 October 2007

Abstract

Peri-cellular remodeling of mesenchymal extracellular matrices is considered a prerequisite for cell proliferation, motility and development. Here we demonstrate that membrane-type 3 MMP, MT3-MMP, is expressed in mesenchymal tissues of the skeleton and in peri-skeletal soft connective tissue. Consistent with this localization, MT3-MMP-deficient mice display growth inhibition tied to a decreased viability of mesenchymal cells in skeletal tissues. We document that MT3-MMP works as a major collagenolytic enzyme, enabling cartilage and bone cells to cleave high-density fibrillar collagen and modulate their resident matrix to make it permissive for proliferation and migration. Collectively, these data uncover a novel extracellular matrix remodeling mechanism required for proper function of mesenchymal cells. The physiological significance of MT3-MMP is highlighted in mice double deficient for MT1-MMP and MT3-MMP. Double deficiency transcends the combined effects of the individual single deficiencies and leads to severe embryonic defects in palatogenesis and bone formation incompatible with life. These defects are directly tied to loss of indispensable collagenolytic activities required in collagen-rich mesenchymal tissues for extracellular matrix remodeling and cell proliferation during embryogenesis.
Published by Elsevier Inc.

Keywords: MT3-MMP; MT1-MMP; Collagenase; Bone formation; Palatogenesis; Cartilage dissolution

Introduction

The collagens are the most abundant components of the extracellular matrix. Present in fibrillar, sheet and mesh-like structures, they constitute the backbone of the diverse extracellular matrices found in tissues of higher animals (Ricard-Blum and Ruggiero, 2005). While essential to extracellular matrix function, the fibrillar collagens are by virtue of their unique molecular properties and mechanical strength also considered to be major physical barriers blocking motility and proliferation of resident cells (Even-Ram and Yamada, 2005; Kuivaniemi et al., 1997; Myllyharju and Kivirikko, 2004; Ushiki, 2002). Most cell types are therefore endowed with efficient enzymatic tools to modulate and degrade peri-cellular collagen matrices, as needed, for unimpeded motility and proliferation during development and homeostasis (Stamenkovic, 2003). Since a major proportion of the fibrillar collagen matrix in bones, teeth and calcified cartilage is amalgamated with biomineral into “hard collagen”, degradation of collagen-rich matrices employs two strategies dictated by whether they are hard or soft. Hard collagen is resorbed by osteoclasts, highly specialized multinuclear cells of the monocyte–macrophage lineage, as they acidify the resorption lacuna between their ruffled border and the mineralized matrix surface and express the potent lysosomal collagen-cleaving enzyme, cathepsin K (Gelb et al., 1996; Goto et al., 2003; Saftig et al., 1998; Teitelbaum, 2000; Vaananen et al., 2000). Despite the absence of mineral, soft fibrillar collagen is an equally tough substrate. Due to its

* Corresponding author. Fax: +1 301 594 1253.
E-mail address: kenn.holmbeck@nih.gov (K. Holmbeck).
[1] Present address: Kingstown Medical College, PO Box 585, Ratho Mill, Saint Vincent.
[2] Present address: NIEHS, MSC E4-09 111 T W Alexander Dr Research Triangle Park, NC 27709, USA.
[3] Present address: The Maurice H. Kornberg School of Dentistry, 3223 North Broad Street, Philadelphia, PA 19140, USA.

0012-1606/$ - see front matter. Published by Elsevier Inc.
doi:10.1016/j.ydbio.2007.10.017

unique architecture, it is essentially impervious to enzymatic breakdown by all but a few select enzymes, working either through receptor-mediated phagocytosis or peri-cellular proteolysis (Engelholm et al., 2003; Everts et al., 1996; Song et al., 2006). Peri-cellular collagenolysis is intimately associated with the true collagenases, so designated not because they are the only collagen-cleaving enzymes, but rather for their ability to cleave the collagen triple helix into characteristic 3/4–1/4 breakdown products at neutral pH and physiological temperature as initially observed in the tadpole tail (Gross and Lapiere, 1962; Gross and Nagai, 1965). The true collagenases belong to the matrix metalloproteinases (MMPs), a subgroup of secreted and membrane-bound or membrane-associated zinc-dependent metalloendopeptidases numbering more than 25 structurally related enzymes with highly variable substrate specificities (Brinckerhoff and Matrisian, 2002; Egeblad and Werb, 2002; Nagase et al., 2006). Of these, membrane-type 1 matrix metalloproteinase (MT1-MMP) functions as a potent peri-cellular collagenase capable of degrading not only soft type I and type II collagen, but also components of the basement membrane such as laminin and type IV collagen (Hotary et al., 2003, 2006; Kadono et al., 1998; Kang et al., 2000; Ohuchi et al., 1997; Sato et al., 1994). MT1-MMP-deficient mice display severe pleiotropic complications arising from the inability to degrade soft type I and type II collagen in mesenchymal tissues (Holmbeck et al., 1999; Zhou et al., 2000). Despite these physical impediments, MT1-MMP-deficient mice survive for a considerable time, suggesting that extracellular matrix breakdown is partially dispensable in early life, achieved by other means such as receptor-mediated phagocytosis, or compensated for by protease-independent strategies for cell motility (Engelholm et al., 2003; Everts et al., 1996; Friedl, 2004). Finally, the deficit in proteolytic capacity may be offset, at least partially, through the activity of other related enzymes. The most obvious candidates to fill this role are the nearest molecular relatives of MT1-MMP in the membrane-bound MMP subgroup. Among these, membrane-type 3 matrix metalloproteinase (MT3-MMP) is closely related to MT1-MMP in molecular structure as well as in expression pattern in dynamically remodeling tissues (Szabova et al., 2005; Takino et al., 1995). We therefore explored the broader function of MT3-MMP in vivo by generating MT3-MMP-deficient mice and subsequently crossing them with MT1-MMP-deficient mice. Here we demonstrate that MT3-MMP is a significant collagenolytic enzyme in vivo which ameliorates the loss of MT1-MMP. Accordingly, MT1-MMP/MT3-MMP double-deficient mice are born with severe developmental defects in collagen-rich tissues, including a severe dysfunction in palatal shelf formation leading to cleft palate. The physiological consequence of double deficiency for MT1-MMP and MT3-MMP is uniform demise of mice shortly after birth caused by morphogenetic defects, which demonstrate for the first time that collagen metabolism in utero is a prerequisite for proper embryonic development. Moreover, these results prove that peri-cellular collagen degradation is governed by at least two cooperating molecules of the membrane-type MMP family, which enable a mechanism in mesenchymal cells required for remodeling of mesenchymal extracellular matrices in the mouse.

Materials and methods

Generation of mice

Laboratory animal experiments in this study were covered under NIDCR approved animal study proposals.

MT3-MMP (Genbank accession # AC_000026) was disrupted by deleting sequences between the *Xba*I site at −728 and the *Bgl*II site at +659 bp relative to the initiation methionine codon. This removes the proximal promoter, exon 1 and part of intron 1 (Fig. 2A). To generate the long arm of the targeting vector construct a 5.5-kb *Hin*dIII subclone was restricted with *Xba*I, blunted with Klenow polymerase and restricted with *Hin*dIII. The resulting 4.6-kb fragment was ligated into pKO 924 (Stratagene, La Jolla, CA) blunt ended at the *Bam*H site and cut with *Hin*dIII. A 0.8-kb short arm was isolated from a 1.6-kb *Hin*dIII subclone with *Pvu*II and *Bgl*II and ligated into pKO 924 cut with *Hpa*I and *Bgl*II.

The targeting vector was electroporated into W4129S6 ES cells (Taconic, Hudson, NY) at 800 V/cm, 200 μF using a 0.4-cm cuvette. G418 resistant clones were screened for the targeted MT3-MMP locus by PCR with primers NeoU1 5′ CCA CTC CCA CTG TCC TTT3′, mt3D1 5′GAC TTA CTA TGC CTC ACC C3′. Agouti offspring were screened by Southern blot on *Hin*dIII digested DNA using a [α-^{32}P]dCTP radio-labeled 0.6-kb intron 1 specific SpeI/*Hin*dIII probe and by PCR using the primers mt3NeoU3 5′CGA CCA CCA AGC GAA ACA3′ and mt3D3 5′GCT CCC AAA GGC ACC ACA3′. The endogenous allele was detected with primers mt3wtU2 5′TGA TGG ATG CCT GGA GAC3′ and mt3wtD2 5′TGC CCA CTG CTG TTG CTA T3′. Genotyping of MT1-MMP deficient mice was done with the primers KH17 5′ACA GAG AAC TTC GTG TTG CCT GAT GAC3′ and 3′16518 5′AGT AGT CGG CGT GGG TGT3′ for the endogenous allele. The targeted allele was detected with the primers KH20 5′GTG CGA GGC CAG AGG CCA CTT GTG TAG CG3′ and Int5 5′AGA TGG AGG AGC AGG AAT GG3′.

Expression of MT3-MMP was assessed by RT-PCR on RNA generated from total neonate tissues. MT3-MMP cDNA was amplified following first strand synthesis with Superscript (Invitrogen, Gaithersburg, MD) with primers MT3ex2 5′AAA TAC GGC TAC CTT CCA CCG ACT GAC CCC3′, Mt3cDNAU4 5′ACC TTC CAC CGA CTG ACC C3′, MT3ex3 5′TCG ATG CGG TGT ACC AGA CCA GAC AAG AGG C3′, MT3ex4 5′ATG CTT ATT TCC CTG GAC CCG GAA TTG GAG GC3′, MT3ex5 5′CCC ACC GCT ATC ATG GCC CCA TTT TAT CAG TAC A3′, Mt3cDNAD4 5′TGC CAC AAG CCT GCT CCT A3′ (Genbank accession # NM_019724). For control of RNA quality, MT1-MMP-specific cDNA was amplified with the primers KH17 5′ ACA GAG ACC TTC GTG TTG CCT GAT GAC3′ and KH 19 5′GAA GAA GTA GGT CTT CCC ATT GGG CAT3′ (Genbank accession # X83536).

Double deficient MT1-MMP/MT3-MMP mice were generated by crossing the MT3-MMP-deficient mice to a mouse strain deficient for MT1-MMP (Holmbeck et al., 1999).

Whole-mount stain of skeletons

Samples were skinned and fixed in 95% EtOH for 24–48 h, eviscerated and incubated in acetone for 24 h, rinsed in water and stained for 96 h in 0.005% alcian blue, 0.015% alizarin red, 5% acetic acid, 70% EtOH. Specimens were cleared in 1% KOH and transferred through graded glycerol solutions and stored in 60% glycerol.

X-ray analysis of mice

Specimens were imaged in a Faxitron MX-20 (Faxitron Corp., Wheeling, IL) with Kodak PPL film (Kodak, Rochester, NY) and exposure for 35 s at 30 kEV.

Histomorphometric analysis

Bone measurements in adult mice were made on X-ray images using NIH image J. Bone length was defined as the longest distance in a straight line from condyle to condyle. Crania were measured on lateral X-ray images as a straight line from the middle of the occipital bone to the tip of the nasal bone.

For cortical bone length of femora and humeri of embryos, the distance between the ends of the cortex on the inner lateral aspect of bones positioned identically was measured.

Recombinant expression of MT3-MMP

The MT3-MMP cDNA was cloned into pWPI (Tronolab). Poly-L-lysine-coated dishes were seeded with 2.5×10^6 293t cells in DMEM, 10% FBS and transfected with pWPI, pSPAX and pVSVG using Lipofectamine Plus (Invitrogen, Gaithersburg, MD). Cells were infected with 0.5 volume of medium from transfected 293t cells and 0.5 volume of fresh medium with 8 μg/ml polybrene.

Cos-7 cells were transfected with mouse MT3-MMP cDNA cloned into pCMVβ (Clontech, Palo Alto, CA) or with empty pCMVβ as a control. The DNA was complexed with GeneJuice (EMD Biosciences, Madison, WI) and the transfection carried out according to the manufacturer's recommendation's.

Collagen breakdown assay

In vitro collagenolytic activity was assessed by plating 5×10^4 cells in 25 μl of DMEM, 10% FBS in the center of a thin film collagen-coated dish. Cos-7 cells were plated at 2.5×10^4 cells per well. Briefly, the collagen film was prepared by neutralization and gelling of acid extracted rat tail tendon collagen (kindly provided by Dr. Jack Windsor). The gel was dried and washed in sterile water as described (Havemose-Poulsen et al., 1998). Attached cells were washed and grown in DMEM, 10^{-9} M IL1β and 10^{-8} M TNFα (Peprotech, Rocky Hill, NJ). Collagenolytic activity was visualized by removing the cells with 0.05% trypsin/EDTA, 1% Triton X-100 and by staining of the collagen with Coomassie blue. Type II collagen films were prepared by sequential coating of wells with 3 mg/ml neutralized acid extracted type II collagen (US Biological, Swampscott, MA). The gels were dried, washed and cells were plated as described above.

Histology

Tissue was fixed in 4% formaldehyde/PBS, decalcified in 0.25 M EDTA/PBS, processed and embedded in paraffin, sectioned at 6 μm and stained with hematoxylin/eosin or used as described in the following sections.

In vivo labeling

Mice were injected IP with 200 mg/kg bromodeoxyuridine (BrdU) (Sigma, St. Louis, MO) in 0.9% w/v sterile saline 1 h prior to euthanasia. Cell proliferation was assessed by reacting sections with a BrdU detection kit (Zymed, South San Francisco, CA) followed by enumeration with NIH Image J.

Detection of apoptotic cells

Apoptotic cells were detected with the Apoptag kit (Chemicon International, Temecula, CA) according to the manufacturers' specifications and enumerated with NIH Image J.

Statistical analysis

Data in Figs. 4B, D, E and Fig. 5I were analyzed by ANOVA one-way test of variance and Tukey's multiple comparison test. Results are given as the mean value±SEM. Data in Figs. 4F and G were analyzed by two-tailed Student's *T*-test and results are given as mean value±SEM.

In situ hybridization

Sections were hybridized to [α-^{33}P]UTP radiolabeled antisense and sense probes specific for MT1-MMP and MT3-MMP as previously described (Szabova et al., 2005).

Real-time PCR analysis

cDNA was amplified with a MyIQ thermocycler and IQ5 software (Bio-Rad, Hercules, CA) initially at 95 °C for 3 min then by 40 cycles of 95 °C for 10 s and 62 °C for 30 s. Melting curves were established by 80 cycles of heating from 55 °C to 95 °C for 10 s. Each sample was analyzed in triplicate twice with threshold levels set automatically. Ct values were normalized to the Ct values for 29S ribosomal protein mRNA. Values were calculated by subtraction of the control expression level from that of the mutant±SEM and analyzed by two factor *T*-test. Primers: MT3-MMP forward: 5′TGA TGG ACC AAC AGA CCG AGA TAA AGA AGG3′, MT3-MMP reverse: 5′GGC CAA GAT GCA GGG AAT GAC AAT AGC3′ (Genbank accession # NM_019724); 29S forward 5′GGA GTC ACC CAC GGA AGT TCG3′, 29S reverse 5′GGA AGC AGC TGG CGG CAC ATG3′ (Genbank accession # BC024393); MT1-MMP forward 5′CCC TCC CTC CAG CCT CCC TTC TC3′, MT1-MMP reverse 5′GAC CGT CTT CTG CTC AGC CCT CAA G3′ (Genbank accession # X83536).

Generation of MT1-MMP-deficient mammary epithelial cells

Mammary glands from 4- to 7-week-old MT1-MMP-deficient and wild-type mice carrying the PymT transgene were explanted in DMEM/F12 (Gibco, Grand Island, NY), 5% FBS, glutamine, penicillin, streptomycin, gentamycin and amphotericin B. Epithelial cells were separated from stromal fibroblasts by brief trypsinization. The procedure was repeated on successive passages of the culture until a pure epithelial population of cells was obtained.

Results

MT3-MMP is co-expressed with MT1-MMP in remodeling tissue

To test the hypothesis that the viability of MT1-MMP-deficient mice, hereafter referred to as "(1 ko)" mice, is due to collagen remodeling by another MT-MMP, we analyzed global *mt3-mmp* expression levels by real-time PCR in collagen-rich tissues of (1 ko) and control wild-type mice. In addition, we established the local *mt3-mmp* pattern of expression by in situ hybridization in (1 ko) mice as well as the *mt1-mmp* and *mt3-mmp* expression patterns in control littermates. The *mt3-mmp* messenger RNA level measured in hind limbs of (1 ko) mice was reduced by 20±9% compared to wild-type control when analyzed by real-time PCR ($N=4$), $p=0.04$. On the local level, in situ hybridization specific for both *mt3-mmp* and *mt1-mmp* demonstrated a substantially overlapping pattern of expression when wild-type mouse femora were analyzed (Figs. 1A, D). Specifically, connective tissue cells lining the bone surfaces of the primary spongiosa in the long bones (Fig. 1A, small arrow) and surfaces of the cortical periosteum (Fig. 1A, arrowheads) displayed expression of both MT1-MMP and MT3-MMP (Figs. 1A, D). Co-expression was also found in the groove of Ranvier (Fig. 1A, large arrow) and, in resting and proliferating chondrocytes albeit with MT3-MMP more abundantly expressed here than MT1-MMP (Figs. 1A, D, asterisks). No appreciable expression was detected in the zone adjacent to the prospective epiphyseal growth plate where hypertrophic chondrocytes reside (Fig. 1A, "HC"), but the region immediately adjacent hypertrophic chondrocytes displayed intense staining for both mRNAs.

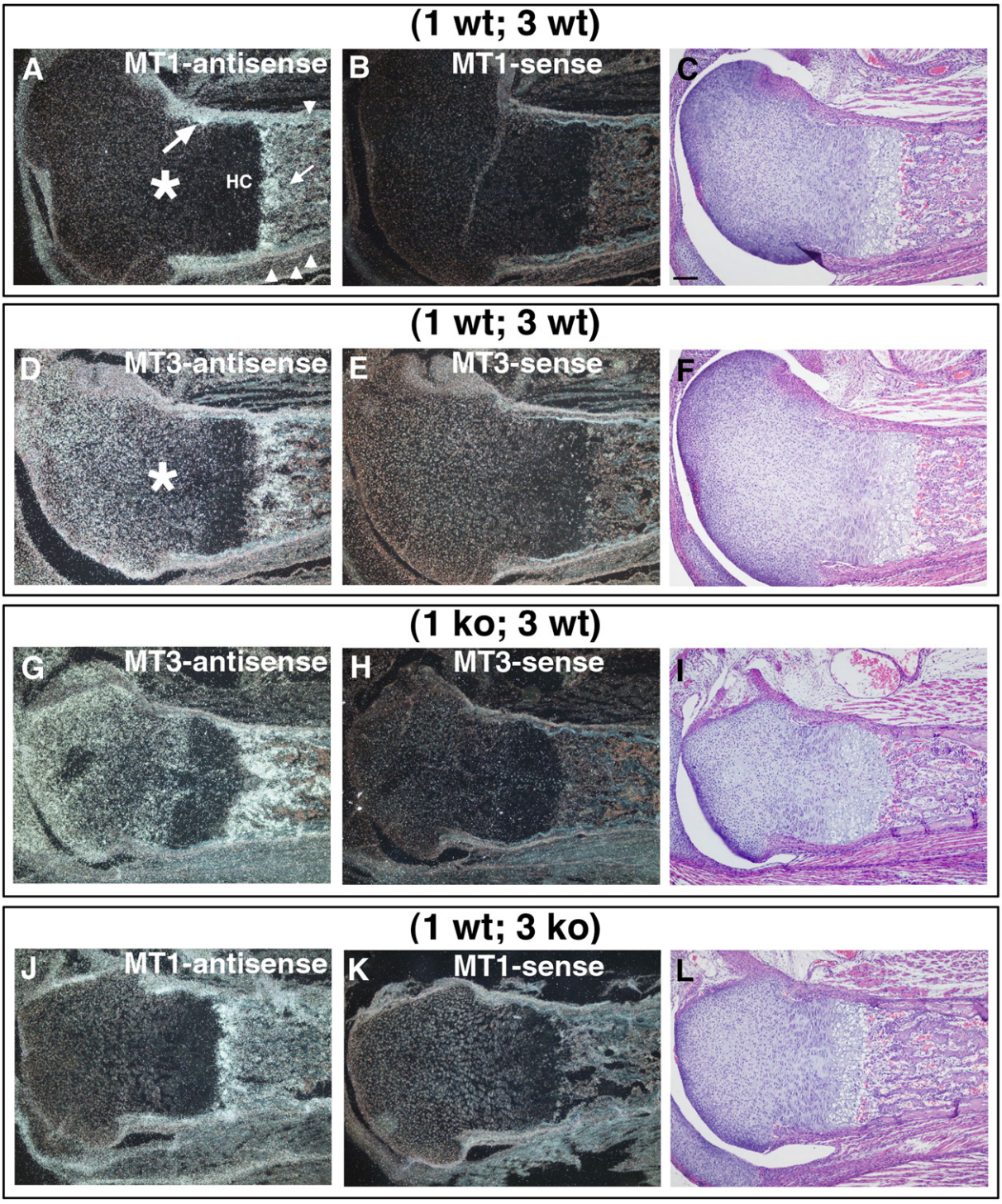

Fig. 1. Expression of MT1-MMP and MT3-MMP in connective tissue, cartilage and bone. Visualization of MT1-MMP and MT3-MMP mRNA expression in the femur and surrounding connective tissue of neonate mice by in situ hybridization on serial sections. (A) MT1-MMP antisense probe hybridized to (1 wt; 3 wt) tissue from neonate mouse. Soft connective tissue (arrowheads) and bone lining surfaces (arrow) display signals for MT1-MMP mRNA with more moderate labeling of the chondrocytes (asterisk). Expression is localized to the groove of Ranvier (large arrow). Hypertrophic chondrocytes (HC) display little staining. (D) MT3-MMP antisense probe localizes to similar areas. Chondrocytes of the condyle display more intense staining than in panel A (asterisk). (G) In the absence of MT1-MMP the distribution of MT3-MMP mRNA is identical to the wild-type expression pattern, compare with panel D. (J) A similar distribution of mRNA is seen for MT1-MMP in the absence of MT3-MMP. (B, K) MT1-MMP sense control hybridizations. (E, H) MT3-MMP sense control hybridizations. (C, F, I and L) Serial sections stained with H&E. Scale bar, C = 100 μm.

When sections from (1 ko) mice were analyzed for the expression pattern of *mt3-mmp* (Fig. 1G) there was no apparent change in the distribution of mRNA compared to wild type (Fig. 1D) that reflected the recorded reduction in global expression established by real-time PCR.

Generation of MT3-MMP deficient mice

Based on the results of in situ hybridization we hypothesized that MT3-MMP played a significant role in mesenchymal cell function. To test this in vivo, we generated mice with a targeted null mutation of the *mt3-mmp* gene (Figs. 2A–B). This mutation effectively ablated the expression of *mt3-mmp* as no messenger RNA from the gene could be detected by a highly sensitive RT-PCR assay (Fig. 2C). Mice homozygous for the *mt3-mmp* null mutation, hereafter referred to as "3 ko", were born in expected Mendelian ratios, were fertile, but displayed retarded growth of the skeleton when compared with either their wild-type (3 wt) or heterozygous (3 +/−) littermates. When global expression of *mt1-mmp* was compared between wild-type mice and 3 ko littermates by real-time PCR, a 37±15% reduction was measured in the 3 ko mice ($N=3$), $p=0.004$. However, the *mt1-mmp* message distribution in the absence of *mt3-mmp* was unchanged (Fig. 1J) when compared to control

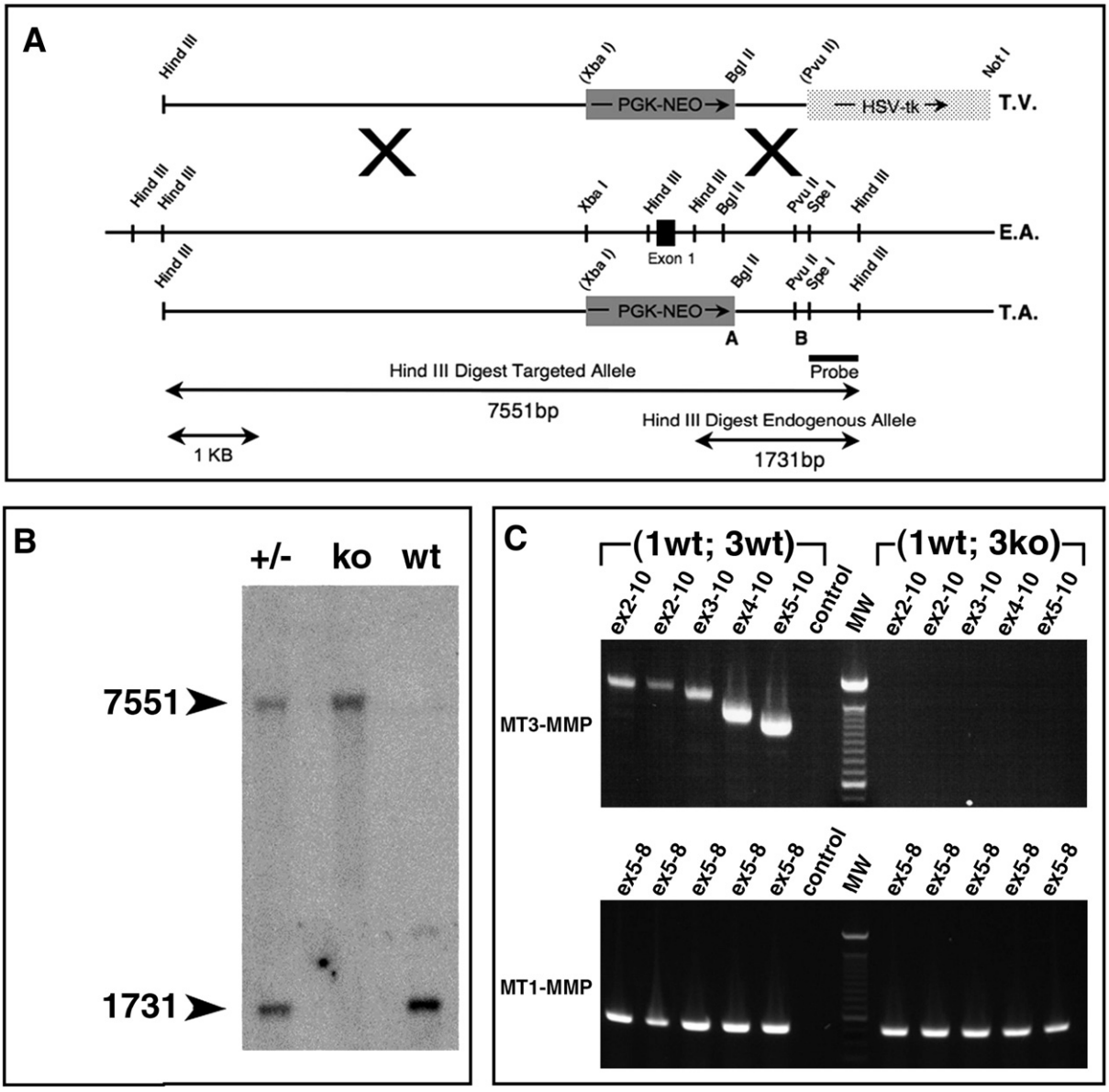

Fig. 2. Targeting of the mouse *mt3-mmp* gene. (A) Strategy for targeting of the mouse *mt3-mmp* gene. T.V.: replacement-type targeting vector using the phosphoglycerate kinase promoter-driven neomycin resistance gene, *PGK-Neo*, solid grey box. The light grey box is the herpes simplex virus thymidine kinase gene, *HSV-tk*, enabling negative selection against random integration of the targeting vector. E.A.: endogenous allele of MT3-MMP with significant restriction endonuclease cleavage sites indicated. Solid black box is exon 1. T.A.: targeted allele, showing exon 1 replaced by the *PGK-Neo* gene. Oligonucleotide primers used for screening of the targeting event indicated by panels A and B. Below is the probe used for Southern blot and the restriction fragments detected by the probe following *Hind*III digest. (B) Southern blot analysis of DNA obtained from tail biopsies from heterozygous (+/−), homozygous mutant (ko) and wild-type (wt) mice. (C) Upper panel: RT-PCR detection of MT3-MMP mRNA in total tissue from wild-type mouse, lanes 1–5 correspond to DNA complementary to exons 2–10, 2–10, second set, 3–10, 4–10 and 5–10, respectively. Lane 6: negative control. Lane 7: molecular weight marker. Lanes 8–12: detection of MT3-MMP mRNA from (3 ko) tissue, note the absence of detectable mRNA for any of the primer combinations used for wild type. Lower panel: lanes 1–5 detection of MT1-MMP-specific mRNA in wild-type tissue. Lane 6 negative control. Lane 7: molecular weight marker. Lanes 8–12: detection of 488-bp MT1-MMP-specific mRNA in (3 ko) tissue.

mice (Fig. 1A). Together with the observations of *mt3-mmp* expression pattern in (1 ko) mice (Fig. 1G), these data suggested that the loss of either MT1-MMP or MT3-MMP did not affect the local expression pattern of the other MT-MMP.

MT1-MMP/MT3-MMP double deficiency leads to perinatal lethality

Given the apparent overlap of MT1-MMP and MT3-MMP we sought to characterize the combined function of these two molecules by the generation of mice doubly deficient for MT1-MMP and MT3-MMP (1 ko; 3 ko). From crosses between (1 +/−; 3 +/−) female and (1 +/−; 3 ko) male mice, offspring of the expected genotype combinations were found at weaning with the exception of (1 ko; 3 ko) and (1 ko; 3 +/−) pups. Monitoring of the litters immediately after birth revealed that a subset of the pups were small, moribund and failed to eat (Fig. 3A). When genotyped, they consistently were (1 ko; 3 ko) mice. Survival recorded from the time of birth revealed that (1 ko; 3 ko) offspring were lower in number than expected and with just one exception, perished within the first day after birth while their (1 ko; 3 +/−) littermates had a median survival of 16 days (Fig. 3D). At weaning, however, all pups with the (1 ko; 3 +/−) genotype had died and only pups of (1 wt; 3 +/−), (1 wt; 3 ko), (1 +/−; 3 +/−) and (1 +/−; 3 ko) genotypes had survived. In contrast, data previously compiled for (1 ko; 3 wt) mice established a 33% demise prior to weaning (Holmbeck et al., 1999) and a subsequent median survival of 60 days for weaned animals. Loss of just one *mt3-mmp* allele thus significantly reduces life span in the absence of MT1-MMP. Furthermore, (1+/−; 3 ko) pups also displayed an increased mortality in the early days after birth and only 80% of these mice survived until weaning (Fig. 3D). Together these results demonstrated that loss of only one *mt3-mmp* allele in the absence of MT1-MMP led to premature death before weaning while combined loss of both genes caused death immediately after birth. In addition to the mortality of the (1 ko; 3 ko) pups, their numbers were smaller than expected. To ascertain if the decreased number of (1 ko; 3 ko) mice was due to intrauterine loss of embryos, several litters were collected at day E 18.5. At that stage of gestation, however, the expected ratio of 12.5% (1 ko; 3 ko) mice was recorded thus establishing that the loss of mice occurred immediately following birth.

Combined MT1-MMP/MT3-MMP deficiency disrupts skeletal development

Analyses of the (1 ko; 3 ko) pups revealed a severe craniofacial dysmorphism over and above that observed in the MT1-MMP deficient mice (Holmbeck et al., 1999). Specifically, the mid-face of the mice was substantially shorter (Fig. 3A) and the skull featured a prominent domed shape, more pronounced than that observed in MT1-MMP-deficient mice (Fig. 3A). In addition, 80% of the (1 ko; 3 ko) pups had prominent clefting of the palates (Fig. 3B, asterisk). The loss of both MT1-MMP and MT3-MMP further resulted in severe stunting of the extremities making (1 ko; 3 ko) pups readily identifiable based on their small limbs (Fig. 3A).

To further characterize the effect of MT1-MMP/MT3-MMP deficiency on skeletal development, we stained skeletons with alcian blue for cartilage and alizarin red for mineralized bone matrix. These whole-mount stained skeletons revealed that the combined loss of *mt1-mmp* and *mt3-mmp* alleles diminished bone formation. In particular, the bone of the cranial vault appeared increasingly thinner with the incremental loss of *mt1-mmp* and *mt3-mmp* alleles. Both the parietal, frontal and nasal bones were poorly developed (Fig. 3C, asterisk). Double deficiency for MT1-MMP and MT3-MMP further affected the formation of cortical bone, specifically in the humeri and femora where a dramatic shortening of the bone cortices could be observed (Figs. 4A, C). This effect, like the effect on skull bones, was proportional to the number of *mt1-mmp* and *mt3-mmp* alleles lost compared to wild type, with the most severe effect observed in the (1 ko; 3 ko) genotype. Measurement of the humoral cortical length at E 18.5 days demonstrated gradual reduction compared to control of 87±0.7% in (1 +/−; 3 ko) pups ($p<0.01$), 83±1.6% in (1 ko; 3 wt) mice ($p<0.001$), 76±4.82% in (1 ko; 3 +/−) mice ($p<0.001$) and 51±4.75% in (1 ko; 3 ko) mice ($p<0.001$) (Figs. 4A, B). Despite diminished early growth compared to wild type, none of the surviving mice displayed a reduction in humerus length at 20 days of age comparable to that observed in (1 ko; 3 wt) mice (Supplemental Fig. 1). However, compared to control mice significant differences were again observed at 30 days of age, where (1 wt; 3 ko) littermate humeri lengths were 92±1% ($p<0.001$), (1 +/−; 3 +/−) humeri were 94±1.2% ($p<0.01$) and (1 +/−; 3 ko) humeri 90±0.7% (Fig. 4E). At 50 days only (1 +/−; 3 +/−) humeri at 93±0.7% of control length ($p<0.05$) and (1 +/−; 3 ko) at 87±1% of control ($p<0.001$) were significantly shorter than control (bar graph not shown).

Femora were likewise shortened in length at E 18.5 to 86±2% of control for (1 +/−; 3 ko) mice ($p<0.01$), 86±1% for (1 ko; 3 wt) mice ($p<0.01$), 74±3.3% for (1 ko; 3 +/−) ($p<0.001$) and 65±2.5% for (1 ko; 3 ko) mice ($p<0.001$) (Figs. 4C, D). In contrast to humeri, femora at 30 days no longer displayed statistically significant reduction in length when compared to control samples (data not shown).

Loss of MT1-MMP and MT3-MMP affects the viability of skeletal cells

The dramatic impairment of long bone formation and cranial bone formation combined with the expression of MT1-MMP and MT3-MMP in both cartilage and bone cells suggested that the reduced availability or outright loss of these two proteolytic enzymes had affected the viability of osteogenic cells and the proliferation of chondrocytes. Enumeration of apoptotic bone-lining cells in femora of newborn mice revealed that loss of MT1-MMP and MT3-MMP imparted a significantly reduced viability dependent on the number of *mt1-mmp* and *mt3-mmp* alleles retained (Fig. 4F, Supplemental Fig. 2). Thus, compared to control (1 +/−; 3 wt) mice the number of apoptotic nuclei in (1 ko; 3 ko) mice was increased 280±70% ($p<0.05$).

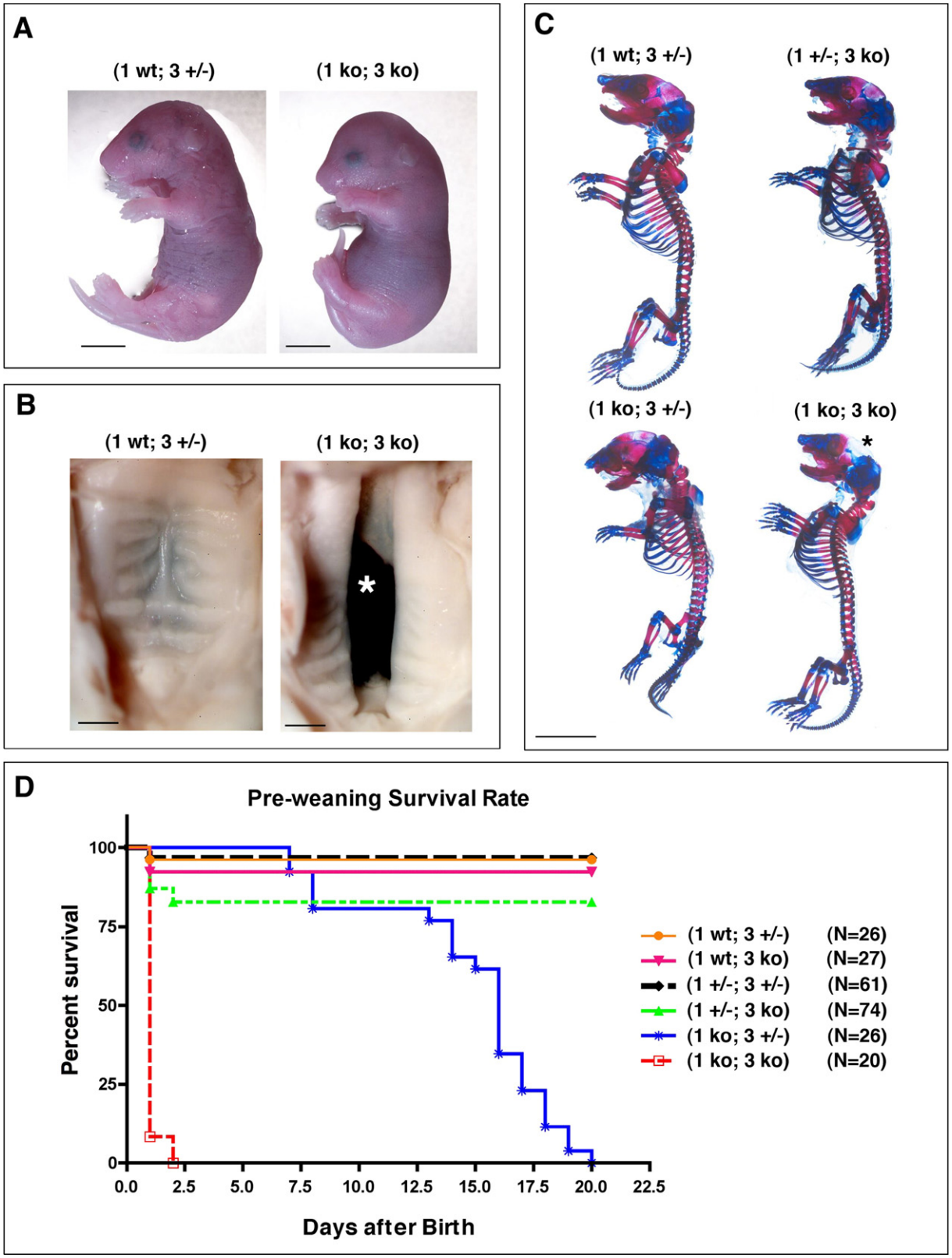

Fig. 3. Combined MT1-MMP/MT3-MMP deficiency leads to severe developmental defects and perinatal death. (A) E 18.5 embryo double deficient for MT1-MMP and MT3-MMP (1 ko; 3 ko) is smaller than the (1 wt; 3 +/−) control. Note the profound dome-shaped head and the short nose and stubby limbs. Scale bar=5 mm. (B) Combined loss of MT1-MMP and MT3-MMP causes incomplete fusion of the palatal shelves and 80% of (1 ko; 3 ko) mice have cleft palate, asterisk in panel B. Scale bar=1 mm. (C) Whole-mount preparation of skeletons from newborn mice stained with alcian blue for detection of cartilage and alizarin red for detection of mineralized bone matrix. The successive loss of *mt1-mmp* and *mt3-mmp* alleles lead to diminished bone formation in the skull, reduction in the cranium size, shortened limbs and reduction in the size of the thorax. Note the virtual absence of the parietal bone in the (1 ko; 3 ko) mice (asterisk). Scale bar=5 mm. (D) Kaplan–Meyer plot of survival of pups prior to weaning.

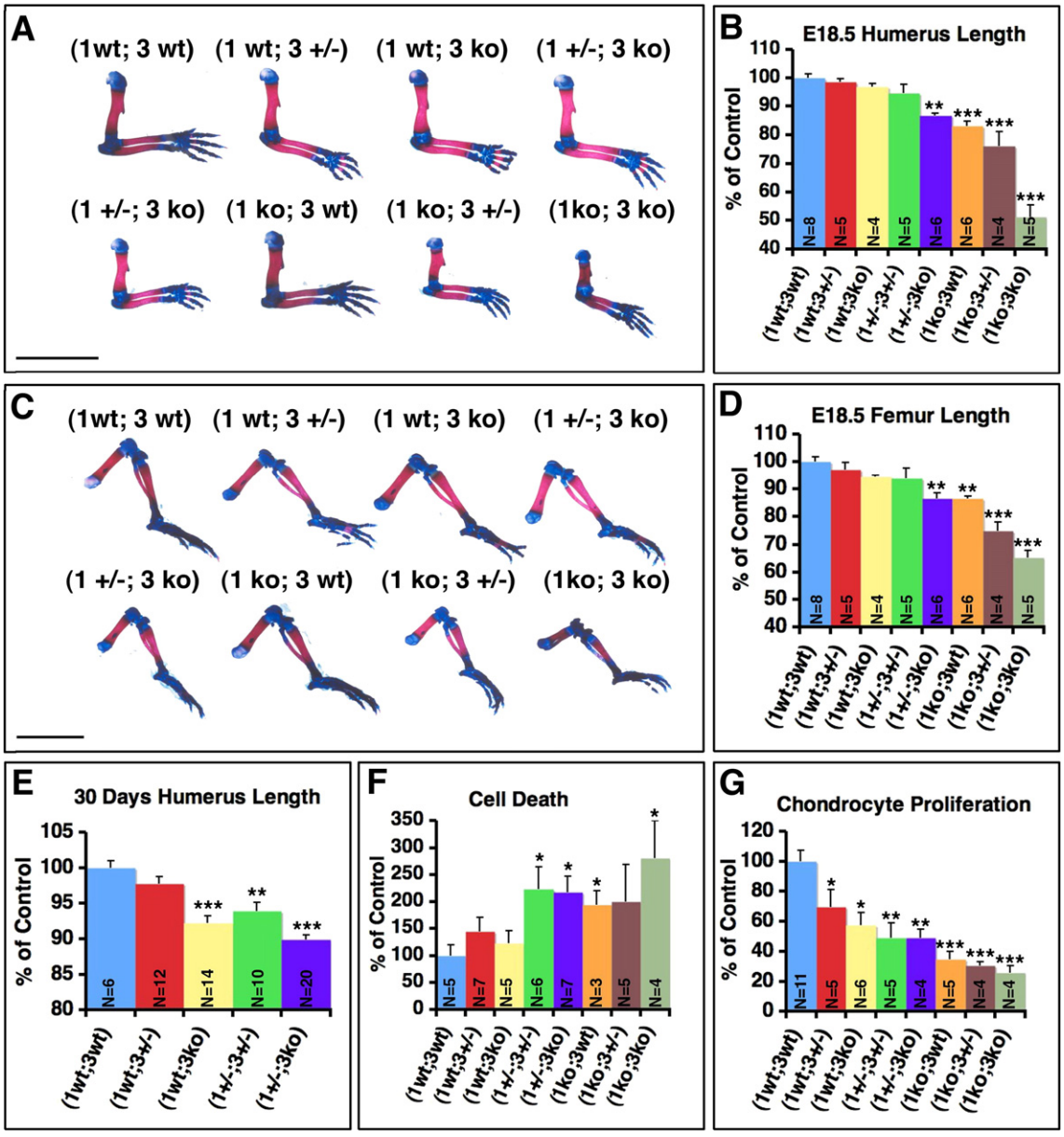

Fig. 4. Combined MT1-MMP/MT3-MMP deficiency leads to embryonic limb deformity, growth retardation and cell demise. (A) Whole-mount preparations of upper extremities from newborn mouse pups stained with alcian blue for cartilage and alizarin red for mineralized bone. The successive loss of *mt1-mmp* and *mt3-mmp* alleles leads to shortening of the long bones in the arm. The formation of the cortical bone is particularly affected and leads to a deformity of the humerus. Scale bar = 5 mm. (B) Length of the humeral cortices in E 18.5 embryos. (C) Whole-mount preparation of lower extremities from E 18.5 embryos. Note the severe impact of combined MT1-MMP/MT3-MMP loss on femoral development. (D) Femoral length at E 18.5. (E) Humeral length at 30 days. (F) Enumeration of apoptotic cells associated with bone surfaces in the distal femoral epiphysis and primary spongiosa of neonate mice. (G) Enumeration of proliferating chondrocytes in the distal femoral epiphysis, zone of proliferating chondrocytes. Bar graphs represent the mean value and error bars indicate standard error of the mean.

Enumeration of proliferating chondrocytes in the distal femoral epiphysis revealed a gradual reduction in cell divisions with the successive loss of alleles, culminating in the (1 ko; 3 ko) mice (Fig. 4G) where only of 25.7±4.8% ($p<0.0001$) of the cell count found in (1 wt; 3 wt) mice was recorded.

Combined MT1-MMP/MT3-MMP deficiency disrupts both intramembranous and endochondral ossification processes

The reduction in bone cell viability and chondrocyte proliferation was consistent with the findings in sections of femora from (1 ko; 3 ko) mice (Figs. 5A–H, Supplemental Fig. 3). Double-deficient mice displayed a markedly elongated zone of hypertrophic chondrocytes (Fig. 5, compare arrows in E vs. F). The core of the primary ossification center where hematopoietic cells normally reside was occupied by a conspicuous island of un-degraded hypertrophic cartilage (Fig. 5H, asterisk) and the zone of proliferating chondrocytes in the epiphysis was marked by a depletion of cells (Fig. 5F, asterisk). In addition to short bone cortices, a striking lack of trabecular bone in the marrow cavity (Fig. 5H) was evident. With the exception of the short cortices, these observations pointed to a deficit in the

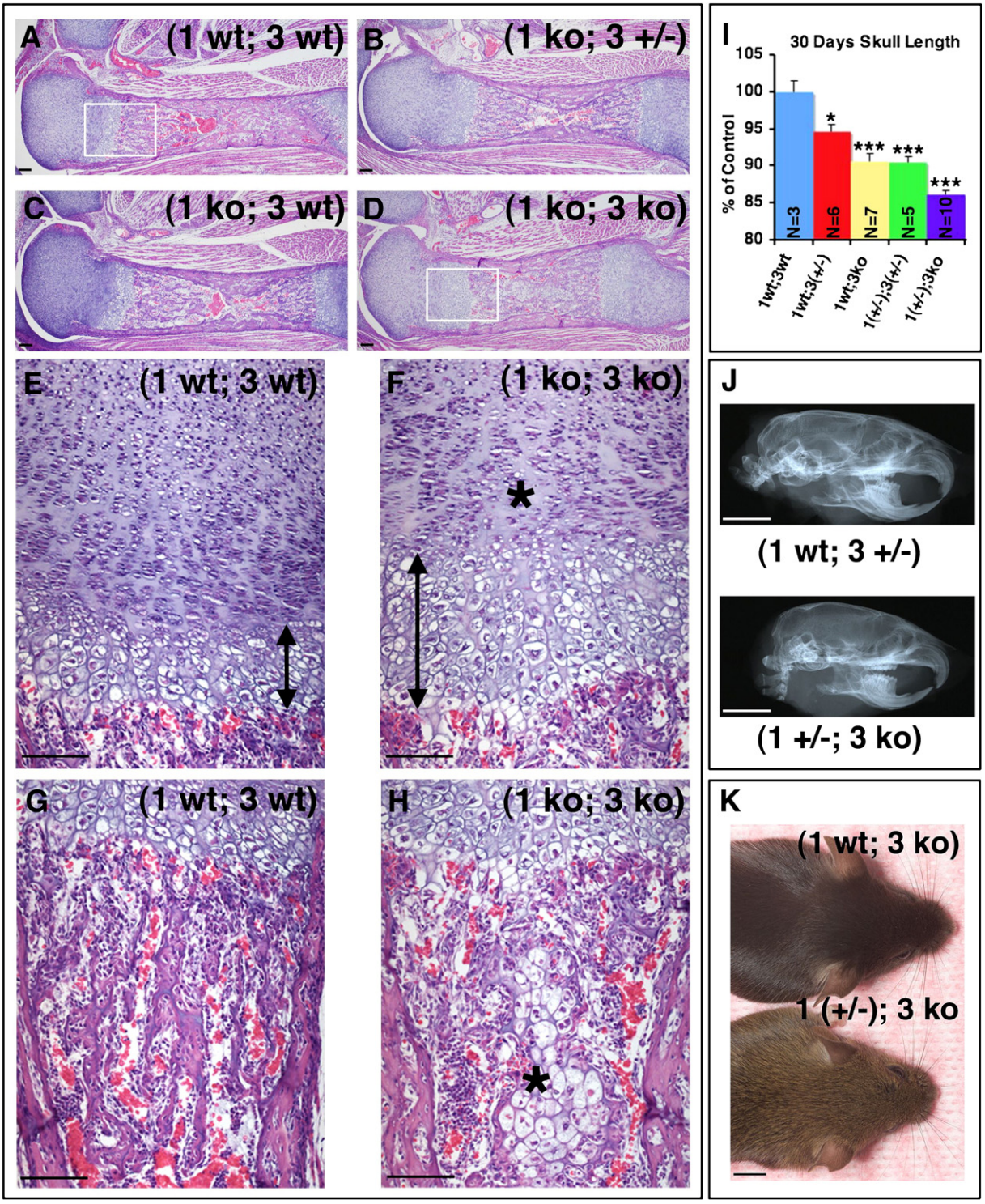

Fig. 5. Combined loss of MT1-MMP and MT3-MMP affects both endochondral and intramembranous ossification. (A–D) Sagittal sections of femora from newborn mice stained with H&E. (A–H) The successive loss of *mt1-mmp* and *mt3-mmp* alleles leads to increasing diminution of longitudinal growth in (1 ko; 3 ko) mice stemming from inability to properly remodel the calcified cartilage and replace it with bone. Boxed areas in panels A and D are shown in higher power magnification below in panels E, G and F, H, respectively. Note the elongated zone of hypertrophic cartilage (compare arrow in E to F) and the reduced number of proliferating chondrocytes (F, asterisk). A conspicuous island of undegraded hypertrophic cartilage remains in the marrow cavity of (1 ko; 3 ko) mice (asterisk, H) and trabecular bone in the primary spongiosa of the (1 ko; 3 ko) mouse is largely absent (compare G vs. H). (I) Measurements of cranium sizes of mice at 30 days. (J, K) Partial loss of MT1-MMP or MT3-MMP affects craniofacial development. (J) X-ray image illustrates how the adult (1 wt; 3 +/−) mice can be differentiated from (1 +/−; 3 ko) mice on the basis of the cranium size and shape at 300 days of age. (K) At 75 days of age the snout of a (1 +/−; 3 ko) mouse is conspicuously shorter compared to that of the (1 wt: 3 ko) littermate. Bar graph in panel I represents the mean value and error bars indicate standard error of the mean. Scale bar, A–H = 100 μm; J, K = 5 mm.

endochondral ossification process not otherwise seen in single-deficient (1 ko) or (3 ko) mice and the likely cause for the shortened and thickened diaphysis (Figs. 5A–C vs. D). In the femur of the (1 ko; 3 +/−) mice, the extended hypertrophic chondrocyte zone and a partially reduced amount of trabecular bone could be observed (Fig. 5B). These defects were, however, less pronounced than those seen in the (1 ko; 3 ko) mice, demonstrating the powerful contribution that just one *mt3-mmp* allele conferred on connective tissue development.

Defective cranial bone formation and palatogenesis in MT1-MMP/MT3-MMP-deficient mice

As suggested by the whole-mount skeletal stains, the loss of MT1-MMP and MT3-MMP significantly affected the growth of the cranium. Initially analysis of mice surviving weaning revealed no overt differences in skull size except for that of (1 ko; 3 wt) mice (Supplemental Fig. 1). However further aging of the mice demonstrated that growth is dependent on MT3-MMP. Accordingly, loss of just one *mt3-mmp* allele significantly reduced cranial size at 30 days (Fig. 5I). Mice thus displayed skull lengths when compared to control mice of 95% for (1 wt; 3 +/−) mice ($p<0.05$), 91% for (1 wt; 3 ko) ($p<0.001$), 91% for (1 +/−; 3 +/−) and 86% for (1 +/−; 3 ko) mice ($p<0.001$). The latter genotype was the most profound in terms of the quantitative reduction in size, but the growth reduction in these mice also affected other aspects of ossification resulting in a unique head shape readily identifiable by an unbiased observer (Figs. 5J, K). Collectively, these data demonstrated that formation of long bone and cortical bone (as well as other intramembranous bones) significantly depended not only on MT1-MMP but also MT3-MMP.

The most severe effect of the deficit in bone formation was seen in the mid-cranium of 1 ko; 3 ko embryos and newborn mice where the formation of the palatine bone was absent (Figs. 6A–F, Supplemental Fig. 4). Upon inspection of serial sections from E 11.5 to E. 15.5 embryos the cause was established to be the reduction of palatal shelf growth and disabled fusion (data not shown). Despite timely elevation of the shelves the lack of growth prevented fusion of the shelves thereby disrupting the formation of the secondary palate in which the osteogenic tissue differentiates. The ensuing ossification of the palatine bone was abrogated, resulting in clefting in 80% of the (1 ko; 3 ko) mice (Fig. 6F). Moreover, the ptygoriod bone was underdeveloped and the maxilla and other mid-cranial bones such as the vomer (Fig. 6D, asterisk) displayed signs of hypoplasia with pitting and lack of fusion to the maxilla (Figs. 6C, D).

In the mandible, individual bone trabeculae of the mutant mice were aberrant and thinner than the control (Figs. 6G, H). Notably, the number of bone lining cells was substantially reduced and the majority of connective tissue cells were instead dispersed between the individual bone trabeculae. Meckel's cartilage was conspicuous in size suggesting the exacerbation of an already impaired cartilage remodeling described previously in MT1-MMP-deficient mice (Holmbeck et al., 2003).

In the cranial vault, the gene deficiency affected intramembranous bone formation (Figs. 6I–J). High power magnification of the parietal bone near the sagittal suture revealed that the bone of (1 ko; 3 ko) mice was abnormal and contained azurophilic patches uncommon in normal bone matrix (Fig. 6J, arrow).

MT3-MMP is a peri-cellular collagenolytic enzyme

The most prominent indication that substrates of MT1-MMP and MT3-MMP are identical is that *mt3-mmp*, when expressed from only one allele, facilitates survival of the mice during most of the pre-weaning period. To test this notion mechanistically, we employed a semi-quantitative collagen degradation assay (Holmbeck et al., 1999). We infected MT1-MMP-deficient (collagenase insufficient) immortalized mammary epithelial cells with an *mt3-mmp* lentiviral expression vector or an empty vector as negative control. As a positive control, we used immortalized MT1-MMP-sufficient mammary epithelial cells. After plating on a high-density fibrillar type I collagen substratum, MT1-MMP-sufficient cells extensively degraded the underlying collagen following stimulation of collagen breakdown (Fig. 7A). MT1-MMP-deficient cells infected with the empty viral vector predictably failed to degrade the underlying substratum (Fig. 7B). In contrast to prior observations (Chun et al., 2004), MT1-MMP-deficient cells infected with the MT3-MMP expressing virus displayed the most robust collagenolytic activity in the assay thereby proving that MT3-MMP alone was sufficient to degrade high-density fibrillar type I collagen as can MT1-MMP (Fig. 7C). To confirm these results we employed Cos-7 cells for transfection with an MT3-MMP expressing vector or empty vector. When plated on type I collagen matrices as described above these cells likewise demonstrated ability to degrade collagen when expressing MT3-MMP (Supplemental Fig. 5).

Given the abundant evidence of defective cartilage remodeling in the (1 ko; 3 ko) mouse (Figs. 5H, K, Fig. 6H), we also tested if MT3-MMP expressing cells could cleave a type II collagen matrix. MT1-MMP-sufficient cells indeed proved capable of degrading the matrix although with less efficiency than they degraded type I collagen (Fig. 7D). MT1-MMP deficient cells again proved incapable of degrading the underlying type II collagen matrix. However, when MT1-MMP-deficient cells infected with MT3-MMP expressing virus were plated on type II collagen, lytic zones in the matrix were detected (Fig. 7F).

Together these data demonstrate that the loss of MT3-MMP leads to a deficit in a potent peri-cellular collagenolytic enzyme, which can partially complement the role of MT1-MMP in peri-cellular collagen degradation. Combined with the analysis of MT1-MMP/MT3-MMP double-deficient mice, these data provide compelling evidence for the function of MT3-MMP as a major peri-cellular collagenolytic enzyme in the mouse.

Discussion

Pursuing the hypothesis that MT1-MMP deficiency is abated by a functionally equivalent enzyme, we document here a

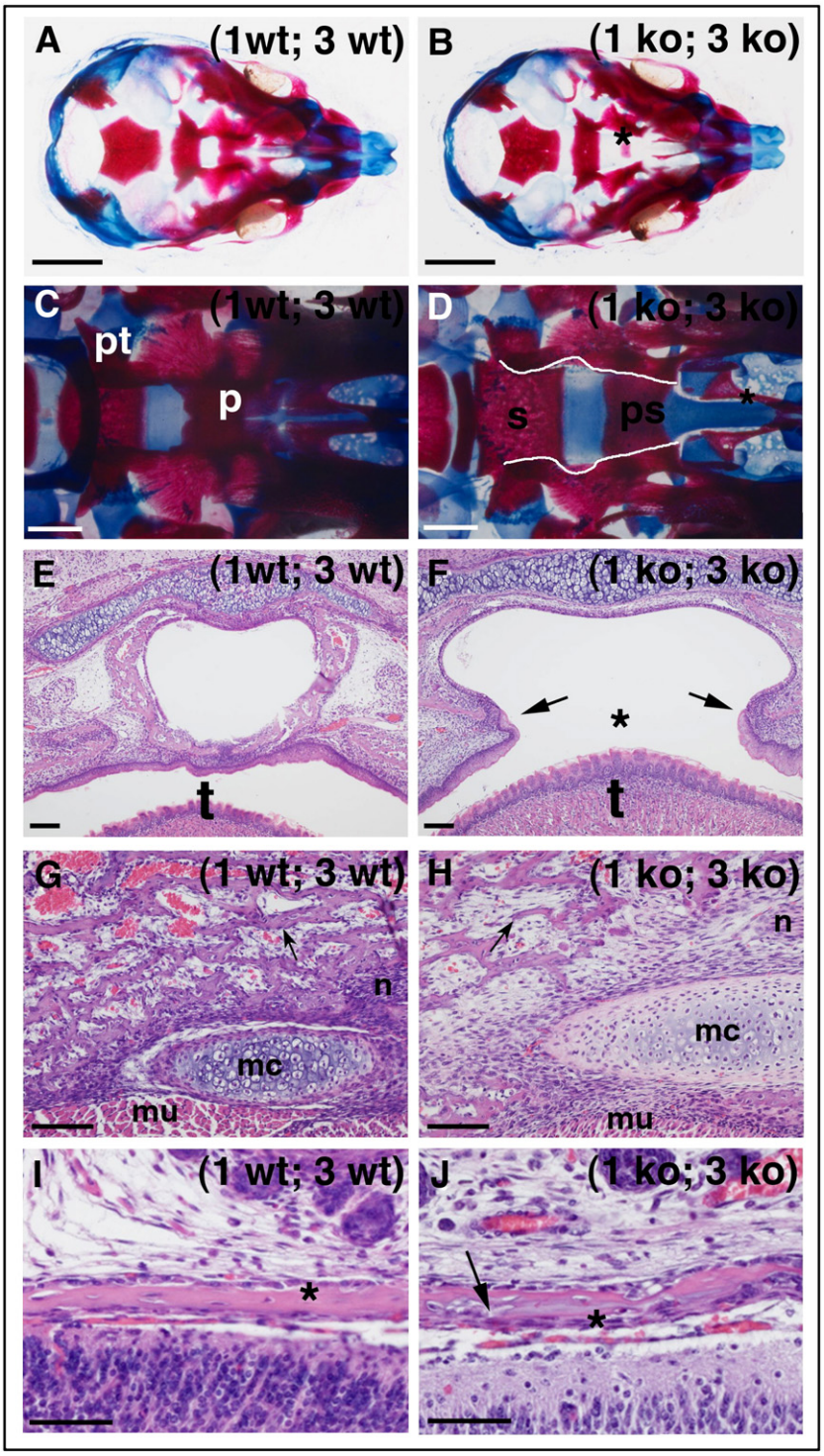

Fig. 6. Combined loss of MT1-MMP and MT3-MMP leads to severe craniofacial developmental defects. (A) Whole-mount (1 wt; 3 wt) cranium stained with alcian blue for cartilage and alizarin red for mineralized bone at E 17.5 and visualized from the base in the absence of the mandible. (B) (1 ko; 3 ko) Littermate displaying a prominent absence of palatine bone fusion, asterisk. (C) Cranium of newborn wild-type mouse showing the fused palatine bone (p) and the ptygoroid bone (pt). (D) The equivalent view of a (1 ko; 3 ko) cranium with overt lack of palatine bone fusion (edges traced by white lines). The unfused palatine bone offers unobstructed view of the sphenoid (s) and pre-sphenoid (ps) bones and the underdeveloped vomer (asterisk). (E, F) Cross-section through the oral cavity and pharynx of newborn littermates. In panel F, the failure to develop the palatal shelves leaves the mouse with a clefted palate, asterisk, above the tongue (t). (G, H) The loss of MT1-MMP and MT3-MMP severely affects the formation of mandibular bone and remodeling of Meckel's cartilage (mc). In panel H, the bone trabeculae are thin and few bone lining cells are found on their surfaces, arrow, compare with G, arrow. The bone is substituted with areas rich in connective tissue cells (mu, muscle; n, nerve). (I, J) In the cranial vault, the bone formation is likewise affected and the parietal bone, asterisks, near the sagittal suture is aberrant looking with azurophilic substance in the matrix (arrow) and irregular surfaces (compare J with I). Scale bars, A, B=2 mm; C, D=0.5 mm; E–H=100 μm; I, J=50 μm.

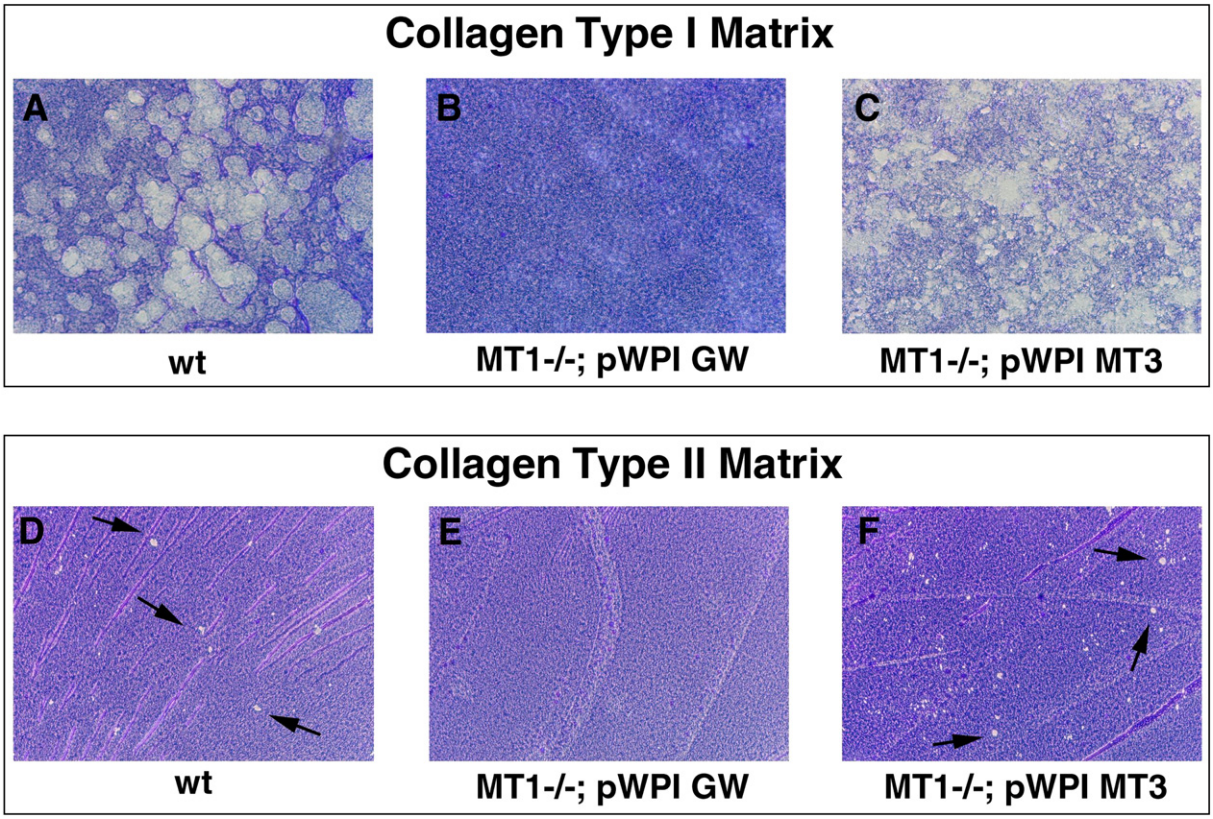

Fig. 7. MT3-MMP is a peri-cellular collagenolytic enzyme. (A) Wild-type (MT1-MP sufficient) cells degrade a high-density fibrillar type I collagen layer when plated on top of this matrix. Following removal of the cells collagenolytic activity is visualized by staining of the matrix with Coomassie blue. Degraded matrix appears as clear lytic zones in the collagen layer. (B) Cells derived from MT1-MMP deficient mice infected with the empty pWPI-GW lentiviral vector display complete inability to degrade collagen. (C) When MT1-MMP-deficient cells are infected with MT3-MMP expressing lentivirus, pWPI MT3, cells regain the ability to cleave fibrillar collagen thus demonstrating that MT3-MMP is a collagenolytic enzyme. Note the robust removal of the matrix by the cells. (D) Wild-type cells also display ability to degrade type II collagen when plated on this matrix (arrows). (E) Loss of MT1-MMP disrupts type II collagen degradation. (F) Expression of MT3-MMP in MT1-MMP-deficient cells restores the ability to degrade type II collagen (arrows).

mechanistic linkage between MT1-MMP and its close molecular relative, MT3-MMP, by the use of mouse genetics.

While the loss of MT3-MMP in itself does not lead to overt physiological deficits, we document an impact on bone formation in the cranium and long bones indicating that MT3-MMP is not merely functionally redundant but required for unimpeded remodeling of extracellular matrix (Figs. 5, 6). Combined with MT1-MMP deficiency, however, it is abundantly clear that loss of either one or two alleles of *mt3-mmp* is associated with a significant exacerbation of the impact of MT1-MMP deficiency in a dosage-dependent manner. The survival of MT1-MMP-deficient mice, despite severe collagen indigestion, originally prompted us to consider if fibrillar collagen metabolism in utero is dispensable for proper development. We demonstrate here that loss of the combined collagenolytic activities associated with MT1-MMP and MT3-MMP is compatible with gestation to term, but with severe developmental defects in appendicular and craniofacial skeleton as consequences. These deficits which affect alimentation and locomotion are associated with uniform perinatal lethality and suggest an absolute requirement for collagen remodeling during development. Furthermore we document that both alleles of MT3-MMP are required for viability past weaning in an MT1-MMP-deficient background.

We observe several effects of combined loss of MT1-MMP and MT3-MMP at the cellular level, which explain the gross phenotypic characteristics encountered in these animals. These observations are distinct from other skeletal deficits associated with the disruption of MMPs (Inada et al., 2004; Itoh et al., 1997; Mosig et al., 2007; Stickens et al., 2004). The strong effect on both bone and cartilage tissues in this model can be traced to the reduced viability of bone surface-associated cells and the diminished proliferation of chondrocytes observed in the prospective epiphyseal growth plate. These deficits are tied to the loss of two major peri-cellular collagenolytic activities, which enable cells to negotiate the extracellular matrix and facilitate functions such as bone apposition and chondrocyte proliferation. Both these functions are essential for the formation of long bone — a combined product of cortical intramembranous bone apposition and coordinated elongation of the core trabecular bone derived by endochondral ossification. In this process, chondrocytes of the epiphysis in succession undergo proliferation, programmed hypertrophy, calcification and ultimately resorption, thereby leaving behind cartilage cores on which bone matrix is deposited (Ortega et al., 2004; Provot and Schipani, 2005).

The impact of reduced cell proliferation predictably affects longitudinal growth, however, partial or complete MT3-MMP

deficiency in an MT1-MMP-deficient background also affects resorption of calcified cartilage and leads to a retardation of endochondral ossification throughout the skeleton.

This observation is not predated by similar findings in mice with single MT1-MMP deficiency and demonstrates that MT3-MMP alone can support the functions of cells required for essential remodeling steps in endochondral ossification and the ensuing formation of trabecular bone matrix. Because the principal resorption of calcified cartilage is thought to be mediated by osteoclasts, our observations do not immediately fit into the established model of endochondral ossification. However, not all parts of the hypertrophic cartilage zone are mineralized; deposition of mineral is confined to the longitudinal septae between individual chondrocytes while the transverse septae maintain an unmineralized state (Sawae et al., 2003). The transverse septae are therefore not substrates for fully differentiated osteoclasts but are considered to be degraded by cells of a vascular endothelial phenotype associated with the invading vessels (Sawae et al., 2003). MT1-MMP and MT3-MMP are expressed in endothelial cells and we hypothesize, based on our demonstration of type II collagen degradation by both proteinases, that invading vascular cells are capable of degrading the type II collagen-rich matrix in unmineralized transverse septae (Plaisier et al., 2004; Sawae et al., 2003). We have previously described the role of MT1-MMP in degradation of unmineralized cartilage during vascular canal formation, an angiogenic process analogous to transverse septum remodeling (Alvarez et al., 2005; Blumer et al., 2005; Holmbeck et al., 1999; Lutfi, 1970). With the loss of MT3-MMP yet another important molecular tool for unmineralized cartilage dissolution in transverse septae is gone. The access of osteoclasts to the longitudinal septae thereby is obstructed, which in turn retards the resorption of the mineralized cartilage matrix and results in an elongated zone of hypertrophic chondrocytes.

The growth of long bone is not only determined by the rate of chondrocyte proliferation but is also highly dependent on the coordinated elongation of the cortical bone. This process is dependent on both bone apposition and remodeling of the cortex interface with the condylar cartilage at the groove of Ranvier (Ranvier 1873; Shapiro et al., 1977). We have previously demonstrated that timely remodeling of the unmineralized cartilage matrix here is critical for growth of the long bone and inability to remodel the matrix at this site in effect clamps the growth of the cortex and disables bone elongation (Holmbeck et al., 2003). We observe here that exacerbation of the collagen indigestion in the MT1-MMP/MT3-MMP-deficient mice leads to further reduction in this interface remodeling function affecting cortical bone growth even in utero.

The effect on bone formation is also evident in the mandible where bone-lining cells are severely depleted and the bone trabeculae are thin and separated by highly cellular spaces suggesting that cells are arrested in their resident matrix. This phenomenon was previously described in MT1-MMP-deficient mice where scarring and fibrosis ensues from a defective matrix remodeling in bone lining soft connective tissue. However, this is restricted to aged MT1-MMP-deficient mice, whereas a similar observation can be made in neonate MT1-MMP/MT3-MMP-deficient mice. This important connection between soft tissue remodeling and impact on the hard mineralized tissue is also the root cause of defective palatogenesis in MT1-MMP/MT3-MMP-deficient mice. Palatal shelf formation is a combined process of cell proliferation, migration, extensive soft connective tissue remodeling and intramembranous bone formation (Greene and Kochhar, 1973; Hilliard et al., 2005). The defective palatogenesis in MT1-MMP/MT3-MMP-deficient mice stems from diminished growth of the palatal shelves, rather than a defect in their elevation and fusion. This points to an early defect in cell proliferation akin to that observed in the cartilage of double-deficient mice. Notably, the mesenchyme in the prospective palatal shelves is highly enriched for type III collagen — a substrate of MT3-MMP (Morris-Wiman and Brinkley, 1992; Shimada et al., 1999). We hypothesize that the cellular defect in remodeling of the extracellular matrix there, as elsewhere in collagen-rich tissues, leads to the reduction of palatal shelf growth. The subsequent failure to establish the secondary palate eliminates the morphological structure in which an osteogenic mesenchyme ordinarily gives rise to the palatine bone.

In conclusion, our data demonstrate that peri-cellular collagen dissolution in vivo is facilitated through two independent proteolytic enzymes, which cooperatively degrade collagen-rich extracellular matrices essential for development and sustained postnatal viability.

Acknowledgments

We thank Ivan Rebustini, Matt Hoffman, Marian Young and Daniel Martin for their technical assistance and Pamela Robey for critical reading of the manuscript. This work was supported by the DIR, NIDCR of the IRP, NIH. M.S. was supported in part by post-doctoral fellowship funds from the Korea Science and Engineering Foundation (KOSEF).

Appendix A. Supplementary data

Supplementary data associated with this article can be found, in the online version, at doi:10.1016/j.ydbio.2007.10.017.

References

Alvarez, J., Costales, L., Lopez-Muniz, A., Lopez, J.M., 2005. Chondrocytes are released as viable cells during cartilage resorption associated with the formation of intrachondral canals in the rat tibial epiphysis. Cell Tissue Res. 320, 501–507.

Blumer, M.J., Longato, S., Richter, E., Perez, M.T., Konakci, K.Z., Fritsch, H., 2005. The role of cartilage canals in endochondral and perichondral bone formation: are there similarities between these two processes? J. Anat. 206, 359–372.

Brinckerhoff, C.E., Matrisian, L.M., 2002. Matrix metalloproteinases: a tail of a frog that became a prince. Nat. Rev., Mol. Cell Biol. 3, 207–214.

Chun, T.H., Sabeh, F., Ota, I., Murphy, H., McDonagh, K.T., Holmbeck, K., Birkedal-Hansen, H., Allen, E.D., Weiss, S.J., 2004. MT1-MMP-dependent neovessel formation within the confines of the three-dimensional extracellular matrix. J. Cell Biol. 167, 757–767.

Egeblad, M., Werb, Z., 2002. New functions for the matrix metalloproteinases in cancer progression. Nat. Rev., Cancer 2, 161–174.

Engelholm, L.H., List, K., Netzel-Arnett, S., Cukierman, E., Mitola, D.J., Aaronson, H., Kjoller, L., Larsen, J.K., Yamada, K.M., Strickland, D.K.,

Holmbeck, K., Dano, K., Birkedal-Hansen, H., Behrendt, N., Bugge, T.H., 2003. uPARAP/Endo180 is essential for cellular uptake of collagen and promotes fibroblast collagen adhesion. J. Cell Biol. 160, 1009–1015.

Even-Ram, S., Yamada, K.M., 2005. Cell migration in 3D matrix. Curr. Opin. Cell Biol. 17, 524–532.

Everts, V., van der Zee, E., Creemers, L., Beertsen, W., 1996. Phagocytosis and intracellular digestion of collagen, its role in turnover and remodelling. Histochem. J. 28, 229–245.

Friedl, P., 2004. Prespecification and plasticity: shifting mechanisms of cell migration. Curr. Opin. Cell Biol. 16, 14–23.

Gelb, B.D., Shi, G.P., Chapman, H.A., Desnick, R.J., 1996. Pycnodysostosis, a lysosomal disease caused by cathepsin K deficiency. Science 273, 1236–1238.

Goto, T., Yamaza, T., Tanaka, T., 2003. Cathepsins in the osteoclast. J. Electron Microsc. (Tokyo) 52, 551–558.

Greene, R.M., Kochhar, D.M., 1973. Palatal closure in the mouse as demonstrated in frozen sections. Am. J. Anat. 137, 477–482.

Gross, J., Lapiere, C.M., 1962. Collagenolytic activity in amphibian tissues: a tissue culture assay. Proc. Natl. Acad. Sci. U. S. A. 48, 1014–1022.

Gross, J., Nagai, Y., 1965. Specific degradation of the collagen molecule by tadpole collagenolytic enzyme. Proc. Natl. Acad. Sci. U. S. A. 54, 1197–1204.

Havemose-Poulsen, A., Holmstrup, P., Stoltze, K., Birkedal-Hansen, H., 1998. Dissolution of type I collagen fibrils by gingival fibroblasts isolated from patients of various periodontitis categories. J. Periodontal Res. 33, 280–291.

Hilliard, S.A., Yu, L., Gu, S., Zhang, Z., Chen, Y.P., 2005. Regional regulation of palatal growth and patterning along the anterior–posterior axis in mice. J. Anat. 207, 655–667.

Holmbeck, K., Bianco, P., Caterina, J., Yamada, S., Kromer, M., Kuznetsov, S.A., Mankani, M., Robey, P.G., Poole, A.R., Pidoux, I., Ward, J.M., Birkedal-Hansen, H., 1999. MT1-MMP-deficient mice develop dwarfism, osteopenia, arthritis, and connective tissue disease due to inadequate collagen turnover. Cell 99, 81–92.

Holmbeck, K., Bianco, P., Chrysovergis, K., Yamada, S., Birkedal-Hansen, H., 2003. MT1-MMP-dependent, apoptotic remodeling of unmineralized cartilage: a critical process in skeletal growth. J. Cell Biol. 163, 661–671.

Hotary, K.B., Allen, E.D., Brooks, P.C., Datta, N.S., Long, M.W., Weiss, S.J., 2003. Membrane type I matrix metalloproteinase usurps tumor growth control imposed by the three-dimensional extracellular matrix. Cell 114, 33–45.

Hotary, K., Li, X.Y., Allen, E., Stevens, S.L., Weiss, S.J., 2006. A cancer cell metalloprotease triad regulates the basement membrane transmigration program. Genes Dev. 20, 2673–2686.

Inada, M., Wang, Y., Byrne, M.H., Rahman, M.U., Miyaura, C., Lopez-Otin, C., Krane, S.M., 2004. Critical roles for collagenase-3 (Mmp13) in development of growth plate cartilage and in endochondral ossification. Proc. Natl. Acad. Sci. U. S. A. 101, 17192–17197.

Itoh, T., Ikeda, T., Gomi, H., Nakao, S., Suzuki, T., Itohara, S., 1997. Unaltered secretion of beta-amyloid precursor protein in gelatinase A (matrix metalloproteinase 2)-deficient mice. J. Biol. Chem. 272, 22389–22392.

Kadono, Y., Shibahara, K., Namiki, M., Watanabe, Y., Seiki, M., Sato, H., 1998. Membrane type 1-matrix metalloproteinase is involved in the formation of hepatocyte growth factor/scatter factor-induced branching tubules in Madin-Darby canine kidney epithelial cells. Biochem. Biophys. Res. Commun. 251, 681–687.

Kang, T., Yi, J., Yang, W., Wang, X., Jiang, A., Pei, D., 2000. Functional characterization of MT3-MMP in transfected MDCK cells: progelatinase A activation and tubulogenesis in 3-D collagen lattice. FASEB J. 14, 2559–2568.

Kuivaniemi, H., Tromp, G., Prockop, D.J., 1997. Mutations in fibrillar collagens (types I, II, III, and XI), fibril-associated collagen (type IX), and network-forming collagen (type X) cause a spectrum of diseases of bone, cartilage, and blood vessels. Human Mutat. 9, 300–315.

Lutfi, A.M., 1970. Mode of growth, fate and functions of cartilage canals. J. Anat. 106, 135–145.

Morris-Wiman, J., Brinkley, L., 1992. An extracellular matrix infrastructure provides support for murine secondary palatal shelf remodelling. Anat. Rec. 234, 575–586.

Mosig, R.A., Dowling, O., DiFeo, A., Ramirez, M.C., Parker, I.C., Abe, E., Diouri, J., Aqeel, A.A., Wylie, J.D., Oblander, S.A., Madri, J., Bianco, P., Apte, S.S., Zaidi, M., Doty, S.B., Majeska, R.J., Schaffler, M.B., Martignetti, J.A., 2007. Loss of MMP-2 disrupts skeletal and craniofacial development and results in decreased bone mineralization, joint erosion and defects in osteoblast and osteoclast growth. Hum. Mol. Genet. 16, 1113–1123.

Myllyharju, J., Kivirikko, K.I., 2004. Collagens, modifying enzymes and their mutations in humans, flies and worms. Trends Genet. 20, 33–43.

Nagase, H., Visse, R., Murphy, G., 2006. Structure and function of matrix metalloproteinases and TIMPs. Cardiovasc. Res. 69, 562–573.

Ohuchi, E., Imai, K., Fujii, Y., Sato, H., Seiki, M., Okada, Y., 1997. Membrane type 1 matrix metalloproteinase digests interstitial collagens and other extracellular matrix macromolecules. J. Biol. Chem. 272, 2446–2451.

Ortega, N., Behonick, D.J., Werb, Z., 2004. Matrix remodeling during endochondral ossification. Trends Cell Biol. 14, 86–93.

Plaisier, M., Kapiteijn, K., Koolwijk, P., Fijten, C., Hanemaaijer, R., Grimbergen, J.M., Mulder-Stapel, A., Quax, P.H., Helmerhorst, F.M., van Hinsbergh, V.W., 2004. Involvement of membrane-type matrix metalloproteinases (MT-MMPs) in capillary tube formation by human endometrial microvascular endothelial cells: role of MT3-MMP. J. Clin. Endocrinol. Metab. 89, 5828–5836.

Provot, S., Schipani, E., 2005. Molecular mechanisms of endochondral bone development. Biochem. Biophys. Res. Commun. 328, 658–665.

Ranvier, L., 1873. Quelques faits relatifs au développment du tissu osseux. Comptes Rendus Acad. Sci. 77, 1105–1109.

Ricard-Blum, S., Ruggiero, F., 2005. The collagen superfamily: from the extracellular matrix to the cell membrane. Pathol. Biol. (Paris) 53, 430–442.

Saftig, P., Hunziker, E., Wehmeyer, O., Jones, S., Boyde, A., Rommerskirch, W., Moritz, J.D., Schu, P., von Figura, K., 1998. Impaired osteoclastic bone resorption leads to osteopetrosis in cathepsin-K-deficient mice. Proc. Natl. Acad. Sci. U. S. A. 95, 13453–13458.

Sato, H., Takino, T., Okada, Y., Cao, J., Shinagawa, A., Yamamoto, E., Seiki, M., 1994. A matrix metalloproteinase expressed on the surface of invasive tumour cells. Nature 370, 61–65.

Sawae, Y., Sahara, T., Sasaki, T., 2003. Osteoclast differentiation at growth plate cartilage-trabecular bone junction in newborn rat femur. J. Electron Microsc. (Tokyo) 52, 493–502.

Shapiro, F., Holtrop, M.E., Glimcher, M.J., 1977. Organization and cellular biology of the perichondrial ossification groove of ranvier: a morphological study in rabbits. J. Bone Jt. Surg. Am. 59, 703–723.

Shimada, T., Nakamura, H., Ohuchi, E., Fujii, Y., Murakami, Y., Sato, H., Seiki, M., Okada, Y., 1999. Characterization of a truncated recombinant form of human membrane type 3 matrix metalloproteinase. Eur. J. Biochem. 262, 907–914.

Song, F., Wisithphrom, K., Zhou, J., Windsor, L.J., 2006. Matrix metalloproteinase dependent and independent collagen degradation. Front. Biosci. 11, 3100–3120.

Stamenkovic, I., 2003. Extracellular matrix remodelling: the role of matrix metalloproteinases. J. Pathol. 200, 448–464.

Stickens, D., Behonick, D.J., Ortega, N., Heyer, B., Hartenstein, B., Yu, Y., Fosang, A.J., Schorpp-Kistner, M., Angel, P., Werb, Z., 2004. Altered endochondral bone development in matrix metalloproteinase 13-deficient mice. Development 131, 5883–5895.

Szabova, L., Yamada, S.S., Birkedal-Hansen, H., Holmbeck, K., 2005. Expression pattern of four membrane-type matrix metalloproteinases in the normal and diseased mouse mammary gland. J. Cell. Physiol. 205, 123–132.

Takino, T., Sato, H., Shinagawa, A., Seiki, M., 1995. Identification of the second membrane-type matrix metalloproteinase (MT-MMP-2) gene from a human placenta cDNA library. MT-MMPs form a unique membrane-type subclass in the MMP family. J. Biol. Chem. 270, 23013–23020.

Teitelbaum, S.L., 2000. Bone resorption by osteoclasts. Science 289, 1504–1508.

Ushiki, T., 2002. Collagen fibers, reticular fibers and elastic fibers. A comprehensive understanding from a morphological viewpoint. Arch. Histol. Cytol. 65, 109–126.

Vaananen, H.K., Zhao, H., Mulari, M., Halleen, J.M., 2000. The cell biology of osteoclast function. J. Cell. Sci. 113 (Pt. 3), 377–381.

Zhou, Z., Apte, S.S., Soininen, R., Cao, R., Baaklini, G.Y., Rauser, R.W., Wang, J., Cao, Y., Tryggvason, K., 2000. Impaired endochondral ossification and angiogenesis in mice deficient in membrane-type matrix metalloproteinase I. Proc. Natl. Acad. Sci. U. S. A. 97, 4052–4057.